#### **REGULAR ARTICLE**



## Substances for regenerative wound healing during antler renewal stimulated scar-less restoration of rat cutaneous wounds

Qianqian Guo<sup>1</sup> · Zhen Liu<sup>1</sup> · Junjun Zheng<sup>1</sup> · Haiping Zhao<sup>1</sup> · Chunyi Li<sup>2</sup>

Received: 1 February 2021 / Accepted: 7 July 2021 © The Author(s), under exclusive licence to Springer-Verlag GmbH Germany, part of Springer Nature 2021

#### Abstract

Scarification is the outcome of cutaneous wound healing under normal conditions. Although considerable effort has been expended in this field, scar-less healing has not been achieved satisfactorily. The lack of a good model of scar-free healing has contributed to this undesirable situation. However, the annual regeneration of deer antlers, which starts from regenerative wound healing over the top of the pedicles (permanent bony protuberances), may provide such a model. Therefore, in this study, we investigated the process of pedicle wound healing at the organ, tissue, cell, and molecular levels. Our results convincingly demonstrate that wounds over the pedicle preceded a regenerative healing process including regeneration of skin appendages, such as hair follicles. Compared to the scar healing in rats, regenerative healing of the pedicle wound exhibited a weaker inflammatory response, lack of myofibroblast induction, and higher ratios of Col III/Col I, TGF-β3/TGF-β1, and MMP/TIMP. Importantly, our periosteal transplantation experiments in vivo revealed that this regenerative healing process was achieved through induction of antler stem cells (ASCs). Further study showed that this effect of ASCs on regenerative healing was not species-specific but more generic and could be applied to other mammalian species, as injection of ASCs stimulated regenerative healing of full-thickness excisional cutaneous wounds in rats. Overall, our findings show that ASCs may have therapeutic potential in enhancing the quality of wound healing and preventing scar formation in clinical settings.

**Keywords** Antler stem cell  $\cdot$  Wound healing  $\cdot$  Regeneration  $\cdot$  Skin  $\cdot$  Scar-less

#### Introduction

The skin is an intricate structure composed of epidermis, dermis, and skin appendages, providing protection to the underlying organs as a structural and physiological barrier between the external environment and the body (Takeo et al. 2015). As the first line of defense against external insults, the skin is constantly exposed to risk of injury and given that the disruption of the skin can severely impair function, a rapid restorative response is vital to ensure survival of the

- Haiping Zhao zhperic@163.com
- ☐ Chunyi Li lichunyi1959@163.com

Published online: 14 August 2021

- <sup>1</sup> Institute of Special Animal and Plant Sciences, Chinese Academy of Agricultural Sciences (CAAS), Changchun, Jilin 130112, China
- Institute of Antler Science and Product Technology, Changchun Sci-Tech University, Changchun, Jilin 130600, China

organ (Peacock et al. 2015; Clark et al. 2007; Yates et al. 2013). Skin repair yields one of two possible outcomes: (1) scarification (wound heals with a fibrotic scar instead of the original tissue structure), or (2) near-perfect skin regeneration (heals without a scar, and with the original tissue structure essentially restored) (Delorme et al. 2012; Moeini et al. 2020). In mammals, scar formation is the most common outcome after injury (Gurtner et al. 2008). Worldwide, hundreds of millions of people suffer from psychological and physiological distress because of the scarring each year (Seifert et al. 2012; Brown et al. 2008). Hence, understanding as to how to deflect the cutaneous wound repair from scar formation to a regenerative outcome remains a goal for many researchers in the field.

The molecular and cellular mechanisms of wound healing have been studied extensively (Seifert et al. 2012; Eming et al. 2014; Shaw and Martin 2016). However, it is still very difficult to induce perfect skin regeneration instead of scar formation during cutaneous wound healing (Seifert et al. 2012). The lack of a good model of scar-free regenerative wound healing in a natural setting in adult animals (Stoica



et al. 2020; Namazi et al. 2011) has contributed to this undesirable situation. However, the annual regeneration of deer antlers, which starts from regenerative wound healing over the top of the pedicles (permanent bony protuberances), may provide such a model. Deer antlers are the only mammalian organs capable of complete renewal (Li et al. 2009; Price et al. 2005), thus offering a unique opportunity to explore how nature has solved the problem of regeneration of a complex mammalian organ including bone, cartilage, blood vessels, nerves, and full thickness of skin (Goss 1995). The wound is created following casting of the previous hard antler (Kierdorf et al. 2003). The regenerative wound healing is believed to be the prerequisite for normal antler regeneration (Li et al. 2005). In some deer species (North America elk), the wound diameter can exceed 10 cm (Goss 1983), and surprisingly, these huge wounds can heal within 2 weeks, leaving negligible or no trace of scars. This phenomenon is unique among mammals, thus suggesting that this healing mechanism could be of significance for realizing the scarless wound healing in a clinical setting. However, this unique antler model system for regenerative wound healing is not well known in the wound healing research field.

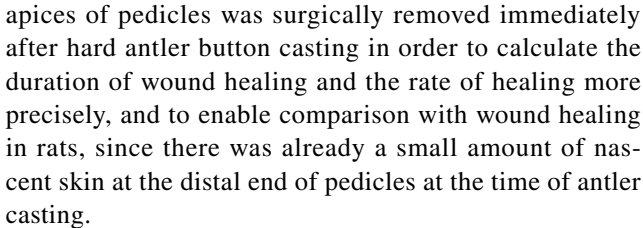
In this study, we took both in vitro and in vivo approaches including different animal models, tissue, cell, and molecular techniques to address the following fundamental questions: (1) whether wound healing over a pedicle stump was regenerative or was just superficially similar; (2) whether the ability for regenerative healing was a feature of the pedicle skin or was acquired through induction of the underlying pedicle periosteum (PP, within which antler stem cells reside); (3) whether induction of the PP for regenerative healing was species-specific or could be expanded to other mammalian species.

Our results convincingly demonstrated that wounds over pedicle stumps executed a process of regenerative healing; induced by the closely adjacent antler stem cell tissue (Li et al. 2009, 2005), antler stem cells could promote full-thickness skin wound healing in a regenerative manner both in deer themselves and in a rat model. Overall, understanding the mechanisms underlying regenerative wound healing underpinned by the antler stem cells could be expected to help greatly in devising effective therapies for scar-less wound healing.

#### **Materials and methods**

#### **Animals**

Seven 3-year-old sika deer (*Cervus nippon*) stags of similar body weight (90–100 kg) were selected for the experiments that involved creation of a pedicle wound and collection of the healing tissue. The nascent skin on the



Male Sprague Dawley (SD) rats (n = 45; 6-week-old; weighing 150 g) were purchased from the Experimental Animal Center of Kunming Medical University. On allocation, full-thickness excisional cutaneous wounds were created in each animal and the animals were divided randomly into three groups: (1) no treatment group (model to compare with pedicle wound healing, n = 15); (2) ASC group (n = 15); and (3) PBS group (control group, used to assess the effect of ASC on wound healing in rats, n = 15).

Animal studies were carried out in strict accordance with the recommendations in the Guide for the Care and Use of Laboratory Animals of the National Institutes of Health and under the approval from the Animal Ethics Committee of Institute of Special Wild Economic Animals and Plants, Chinese Academy of Agricultural Sciences (Permit Number: NO.ISAPSAEC-2020-022). Animals used in this study including deer and rats were housed and bred under standard conditions. Experimental deer were placed together in one barn at least 1 month before start of the study to acclimatize themselves. Rats were kept in a temperature-controlled room (21–24 °C) under a 12:12 light and dark cycle. All animals had free access to water and feed, and were weighed before surgery and at regular intervals subsequently during the experimental period. Surgery was performed under aseptic conditions and under general anesthesia. After surgery, animals were monitored daily to detect odd behavior. The number of animals was reduced to the minimum according to the significant statistical analysis, and animal suffering was minimized based on the experience of 39 years of studies on deer.

### Creation of full-thickness excisional cutaneous (FTE) wounds in rats

All rats were anesthetized with 10% chloral hydrate. Dorsal hair was shaved, and the exposed skin was sterilized with 70% ethanol. One round full-thickness excisional wound was created for each rat with a sterile 12-mm biopsy punch on the dorsal skin between the range of the forelimbs and the hindlimbs. Each rat was housed in an individual cage after surgery. Rats in the ASC group were treated with three subcutaneous injections (25  $\mu$ l/injection) of antler stem cells (1×10<sup>6</sup> cells) in PBS around the wound; rats in the PBS group were treated with three subcutaneous injections of PBS (25  $\mu$ l/injection) around the wound.



#### Collection of the healing skin tissue

One deer was randomly selected for continuous observation, and the remaining six deer (total of 12 pedicles) were randomly divided into two groups (3 deer/group and 6 pedicles/group) for sampling. The healing skin tissues over two pedicle stumps of each deer in one group were respectively sampled on days 1 and 5, and those in the other group were respectively sampled on days 3 and 7 after wound healing. Each skin sample was divided into four parts for histological examination, protein microarray analysis, quantitative real-time PCR, and transcriptome analysis, respectively. Rats were sacrificed on days 3, 7, 14, 21, and 28 post-surgery (n=3 per time point), respectively, and the healing skin tissues were collected for histological analysis. For histological and immunohistochemical examinations, skin tissues were fixed in 10% formalin immediately after removal, embedded in paraffin, and sectioned at 4 µm.

#### Histology

All skin tissue sections were deparaffinized, rehydrated, and stained with hematoxylin and eosin (H&E) for histology examination (Goss 1983). For evaluation of collagen content and pattern, Masson's trichrome (Solarbio, China) and Picrosirius Red staining (Beijing Tian Enze, China) were performed using commercial kits according to the manufacturers' protocols. For Picrosirius Red staining, tissue sections were placed in Picrosirius Red solution for 2 h, washed, and finally stained with hematoxylin for 5 min. Stained sections were then dehydrated, mounted, and then examined and photographed under a light microscope (Nikon, Japan).

For detection of the basement membrane (BM) in the healing skin tissue, periodic acid Schiff (PAS) staining was performed using a PAS staining kit (Solarbio, China) according to the manufacturer's protocol. Briefly, skin tissue sections were placed in the oxidant at room temperature for 5–8 min, washed with PBS, stained in the Schiff reagent in the shade for 15 min, washed with water, stained with hematoxylin for 2 min, rinsed in reagent D, and finally dehydrated. The stained sections were examined and photographed under a light microscope (Nikon, Japan).

### Classification of wound healing phases

Wound healing in mammals has been divided into three distinct but overlapping phases, namely inflammation (I), proliferation (II), and remodeling (III) phases (Reinke and Sorg 2012; Olczyk et al. 2014). In the inflammatory phase, a large number of inflammatory cells infiltrate the wound

area to cleanse the area of bacteria and cell debris (Olczyk et al. 2014); in the proliferation phase, resident cells including fibroblasts are in extensive mitosis to form granulation tissue "closing" the wound gap (Akita 2019; Reinke and Sorg 2012); and in the remodeling phase, both cell proliferation rate and density of fibroblasts in the healing tissue decrease and collagen fibers become thickened and the spatial organization is re-constructed in an attempt to recover normal tissue strength (Reinke and Sorg 2012). Since the wound size and healing rate in rat and deer pedicles were quite different (12-mm and 45-mm diameters, respectively), we matched each sampled tissue from a pedicle wound or from a rat wound to one of these three phases of wound healing defined above, and then made comparisons between the rat and pedicle tissue samples that fell within the same phase of healing.

#### Immunohistochemistry

Immunohistochemistry was performed using an UltraSensitive<sup>TM</sup> SP (Mouse/Rabbit) HC Kit (MX Biotechnologies, China) according to the manufacturer's protocol. Briefly, skin tissue sections were dewaxed, rehydrated, and subjected to antigen retrieval. Thereafter, the sections were washed in PBS, placed in 5% bovine serum albumin to block nonspecific binding to antibodies, and then incubated with primary antibodies overnight at 4 °C, including rabbit anti-L-plastin (1:200, Abcam, ab109124), rabbit anti-a-SMA (1:2000, Abcam, ab32575), rabbit anti-ki67 (1:1000, Abcam, ab16667), rabbit anti-TGF-β3 (1:100, Abcam, ab15537), or mouse anti-TGF-β1 (1:100, Abcam, ab190503). Rabbit IgG (1:500, Abcam, ab172730) was used as isotype control. After 3 washes with PBS, tissue sections were incubated with biotinylated secondary antibody for 10 min at room temperature, and finally visualized using DAB (3,3-diaminobenzidine) (MX Biotechnologies, China). Images were captured under an inverted microscope (Nikon, Japan) or slice scanner (Leica, Germany). We selected 10 random fields per section and 3 sections in total for the quantification of IHC results. The IHC results were analyzed via Image-Pro Plus.

#### Creation of ectopic pedicle wounds

It is known that the periosteum overlying the frontal crest (antlerogenic periosteum, AP) of a male sika deer calf possesses the potential to induce ectopic pedicle and antler formation when subcutaneously transplanted elsewhere on the deer body (Li and Suttie 1994, 2001, 2003; Li et al. 2007). To verify whether the regenerative healing ability of pedicle wounds was an attribute of the pedicle skin or acquired when the skin became associated with pedicle periosteum



(PP), we subcutaneously transplanted the AP tissue to the forehead region, where the skin can form only a scar following wounding. Male sika deer calves (8–9 months) were selected before pedicle initiation to provide AP, the tissue from which the PP directly derives. The detailed procedures for sampling and autologously transplanting AP have been reported elsewhere (Li et al. 2007; He et al. 2018).

### Microarray of inflammatory cytokines and chemokines

Lysates of the skin tissue samples were prepared through homogenization in a Dounce homogenizer containing lysis buffer (Raybiotech, USA), and centrifuged at 13,200 g, at 4 °C for 15 min, and the supernatants collected. Protein content in the supernatant was measured using the BCA Protein Assay kit (Beyotime, China). Then, 100 μl of the supernatant was used for the measurement of cytokines and chemokines using the Quantibody Bovine Cytokine Array 1 (RayBiotech, USA) as per the manufacturer's instructions. The signals were visualized using a microarray scanner (GenePix Professional 4200A, Bucher Biotec AG). Data extraction was performed using GenePix Pro 6.0 software (Axon Instruments, USA).

#### Quantitative real-time PCR (qRT-PCR)

Specific primers in the gene coding regions were designed using Primer 5 software and listed in Table S1. Total RNA was isolated from each tissue sample using Trizol reagent (Invitrogen, Shanghai, China) according to the manufacturer's protocol. RNA quality was assessed using an Agilent 2100 Bioanalyzer (Agilent). Total RNA (1 µg) was reverse-transcribed and the resulting cDNA was used as a template. The qRT-PCR was then performed using the SYBR Kit (Applied Biosystems, Foster City, CA, USA) according to the manufacturer's protocol using the Real-Time PCR Detection System (Roche, Basel, Switzerland). GAPDH was used as an internal control, and all reactions were performed in three biological replicates. The relative quantitative method (2- $\Delta\Delta$ CT) was used to calculate the fold change in expression levels of the target genes (Schefe et al. 2006).

#### RNA-seq

Tissue samples were ground rapidly into fine powder using a Freezer/Mill 6770 (SPEX CertiPrep Ltd., USA). Total RNA was extracted from the sample powder using a Trizol reagent (Invitrogen Inc., Camarillo, CA) according to the manufacturer's procedure. RNA quality was assessed using Bioanalyzer with a minimum RNA integrity number of 7.0. In total,

6 mg of total RNA was used to construct libraries according to the manufacturer's instructions (Illumina TruSeq Library Preparation Kit v3). Libraries were sequenced using an Illumina HiSeq X Ten at BGI (Shenzheng, China). We sequenced three biological replicates with 150-bp paired-end sequencing. The data were analyzed using several bioinformatics software including Metascape (http://metascape.org) platform and Dr.tom software. Statistical analyses for RNA-seq data were performed as previously described (Falcon and Gentleman 2007).

#### **Statistics**

RNA-seq data processing was performed with Cufflinks and R-Studio software. Statistical significance for differentially expressed genes (DEGs) was set at logFC>1 and FDR < 0.01. Statistical analyses for none-RNA-seq data were performed using Prism 8 (GraphPad Software, La Jolla, CA, USA). Quantitative data were presented as mean  $\pm$  standard error of mean (mean  $\pm$  SEM). Statistical analysis for the comparisons of multiple variables was performed using a two-way ANOVA, and Student's t test was used to compare 2 variables. Values were set at p < 0.05 for statistical significance.

#### Results

## Morphological observation of healing course over a pedicle stump wound

Since nascent skin was already present in most cases on the distal end of a pedicle at the time of hard antler button casting, the rim of the distal pedicle skin was removed immediately after casting of a button. The resulting wound was the combined area of the casting surface and the bare area following removal of the rim tissue and averaged about 45 mm in diameter; see Fig. 1a, b. In response to injury, blood rapidly flowed onto the wound bed but clotted in minutes and formed a scab. The healing skin grew centripetally over a pedicle stump, encircling the scab, and no wound contraction was observed (Fig. 1b-e). During the period of the experiment, no signs of infection or inflammation were detected at the wound site at any time (i.e., no sign of redness or swelling around the wound). The scab remained in the center of a pedicle stump wound until no later than day 10, when the wound had healed completely (Fig. 1e). At about this time, the scab flicked off and the wound healing was morphologically completed. A sparse population of fine hairs on the healed skin was observed, indicating the nature of velvet skin (Fig. 1e).



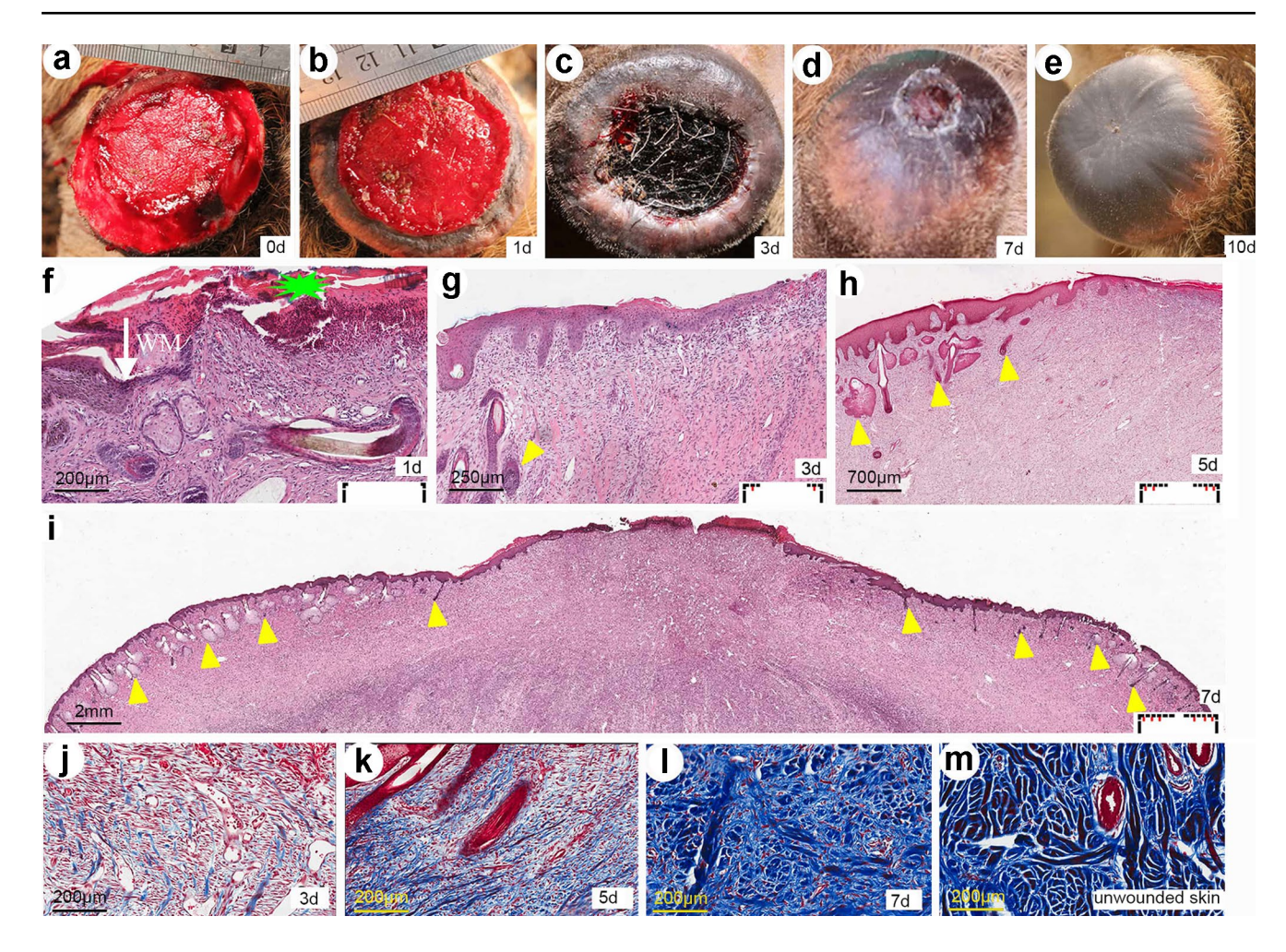


Fig. 1 Morphological (a-e) and histological (f-m) observations of the course of healing over a pedicle stump cutaneous wound. The average size of resulting pedicle wound was about 45 mm in diameter (a). The healing skin grew centripetally over a pedicle stump, encircling the scab (b-d). Around day 10 after initial wounding, healing was morphologically completed (e). Skin samples were collected at different time points (f-i) over the course of pedicle wound healing. Day 1 (f), blood rapidly flowed onto the wound bed, clotted, and formed a scab (green asterisk); inflammatory cells infiltrated under the scab (WM, wound margin). Day 3 (g), the number of dermal cells in the healing skin was increased, the migrating epidermis had already covered a significant portion of the wound area together with dermal tissue, and there were hair follicles and sebaceous glands (yellow arrowheads) on the wound bed. Day 5 (h), numerous appendages

were apparent in the healing skin. Day 7 (i), around 80% of healing had been completed. Extracellular matrix (density and pattern) over the course of healing of a pedicle wound via Masson's trichrome staining (j-m). Collagen fibers were stained blue and cells are stained red. Day 3 (j), thin collagen fibers were present and a large number of cells evident in the healing skin. Day 5 (k), collagen fibers are thickened and increased in number. Day 7 (l), abundant collagen fibers were evident and exhibited a basket-weave-like pattern, and the number of dermal cells was decreased. Collagen pattern of the unwounded pedicle skin (m). Insets in f-i indicate the progression of wound healing: dotted line, new skin; short red line, newly formed glands. Scale bars = 200  $\mu$ m (f), 250  $\mu$ m (g), 700  $\mu$ m (h), 2 mm (i), and 200  $\mu$ m (j-m) respectively

### Pedicle stump wounds heal through a regenerative manner

Histological examination of healing edge tissue of the wound over a pedicle stump was carried out to reveal the nature of wound healing. On day 1 after creation of a pedicle wound, a blood scab was seen covering the wound site; under the scab, inflammatory cells had infiltrated, and epithelial cells from the wound margins were in proliferation

mode and had started to migrate under the scab for reepithelialization (Fig. 1f). By day 3, there was evidence of significant centripetal movement of the newly formed epidermis. The wound epithelium was 8 to 10 cells in thickness, and rich in large rete pegs that had formed along the basal layer of healing epidermis and that had moved deeply into underlying dermis. The number of dermal cells in the wound bed increased, including both fibroblasts and endothelial cells. Newly deposited extracellular matrix



(ECM) was seen (Fig. 1g, j). Along with the progression of re-epithelialization, hair follicles and sebaceous glands were formed. By day 5, epidermal cells had continued to migrate in the process of re-epithelialization, collagen fibers had increased in number, and more hair follicles and sebaceous glands were found in the healing skin (Fig. 1h, k). By day 7, around 80% of the healing was achieved. Cell density had decreased significantly in the healing tissue. The total collagen content increased, with collagen having been reconstructed and rearranged in a basket-weave-like pattern (Fig. 1l), resembling an intact undamaged dermis (Fig. 1m).

Numerous regenerated appendages were adorned in the healing skin, and the pattern of dividing cells showed that the process of hair follicle regeneration resembled that of hair follicle development (Fig. 2). Thus, our conclusion is that the histological structure of the healing skin on a pedicle stump wound resembles that of normal skin, including hair follicles and sebaceous glands, but absent any sign of tissue fibrosis. Our histological results show that healing of a pedicle wound is a regenerative process.

## Pedicle regenerative healing exhibits impaired inflammatory response and lacks myofibroblast differentiation compared to rat wounds

We examined the inflammatory response to wounding in the healing tissues over pedicle stump and rat cutaneous wounds through IHC staining. L-Plastin (pan-leukocytic marker) staining showed (Fig. 3a–f) that an influx of leukocytes was

observed at phase I after wounding in both cases. However, the change in number of leukocytes was not significant over the entire course of wound healing in pedicle wounds, whereas as wound healing progressed in the rats, the number of leukocytes decreased significantly. At phase II, leukocytes were significantly decreased and at phase III leukocytes were hardly detectable. Statistical analysis of the phase I data showed that the number of leukocytes was significantly lower (p < 0.001) in the pedicle than that in rats at the time when leukocyte numbers in both pedicle and rat were at their peak (Fig. 3g).

Staining with  $\alpha$ -smooth muscle actin ( $\alpha$ -SMA), a marker for myofibroblasts, showed that no specific signals were detected in the healing tissue at different time points over a pedicle stump wound, and the specific staining was mainly localized to the wall of blood vessels (Fig. 3h–j), as  $\alpha$ -SMA is also the marker of blood vessel wall. In contrast, strong specific staining for myofibroblasts was detected in the rat wounds (Fig. 3k–m), especially at phase II. Together, these results indicate that there is a significant difference in wound healing contraction between the pedicle stump and rat cutaneous wounds, noting also that the pedicle wound healing lacks any evidence of contraction.

### Pedicle regenerative healing formed more type III collagen and did not delay BM regeneration

Type I collagen (Col I) and type III collagen (Col III) fibers were detected differentially via Picrosirius red staining under a polarized light microscope. The results showed a

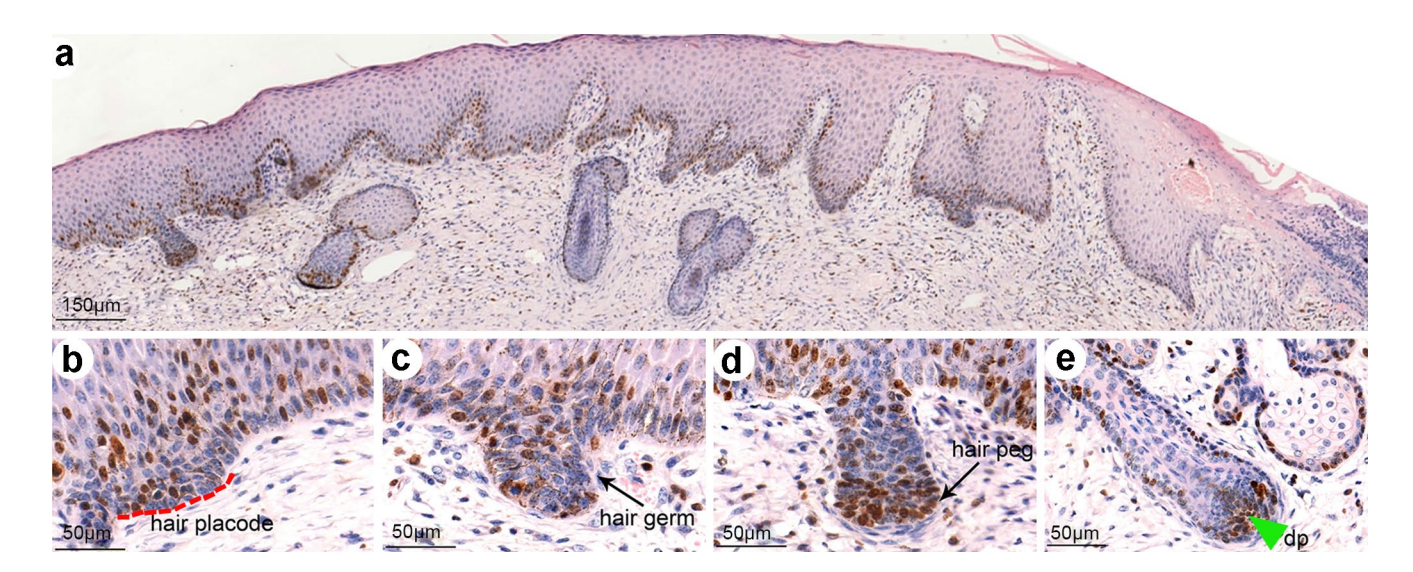


**Fig. 2** Regeneration of hair follicles during cutaneous wound healing over a pedicle stump. **a–b** KI67-labeled cells (brown, proliferating). Note that numerous cells were labeled but mainly located in the basal layer of newly formed epidermis (**a**). Higher magnification (**b–e**) of

**a** to enable a closer examination at hair placode, hair germ, and hair peg, and in the dermal papilla (dp). Scale bars = 150  $\mu$ m (a), 50  $\mu$ m (b-e)



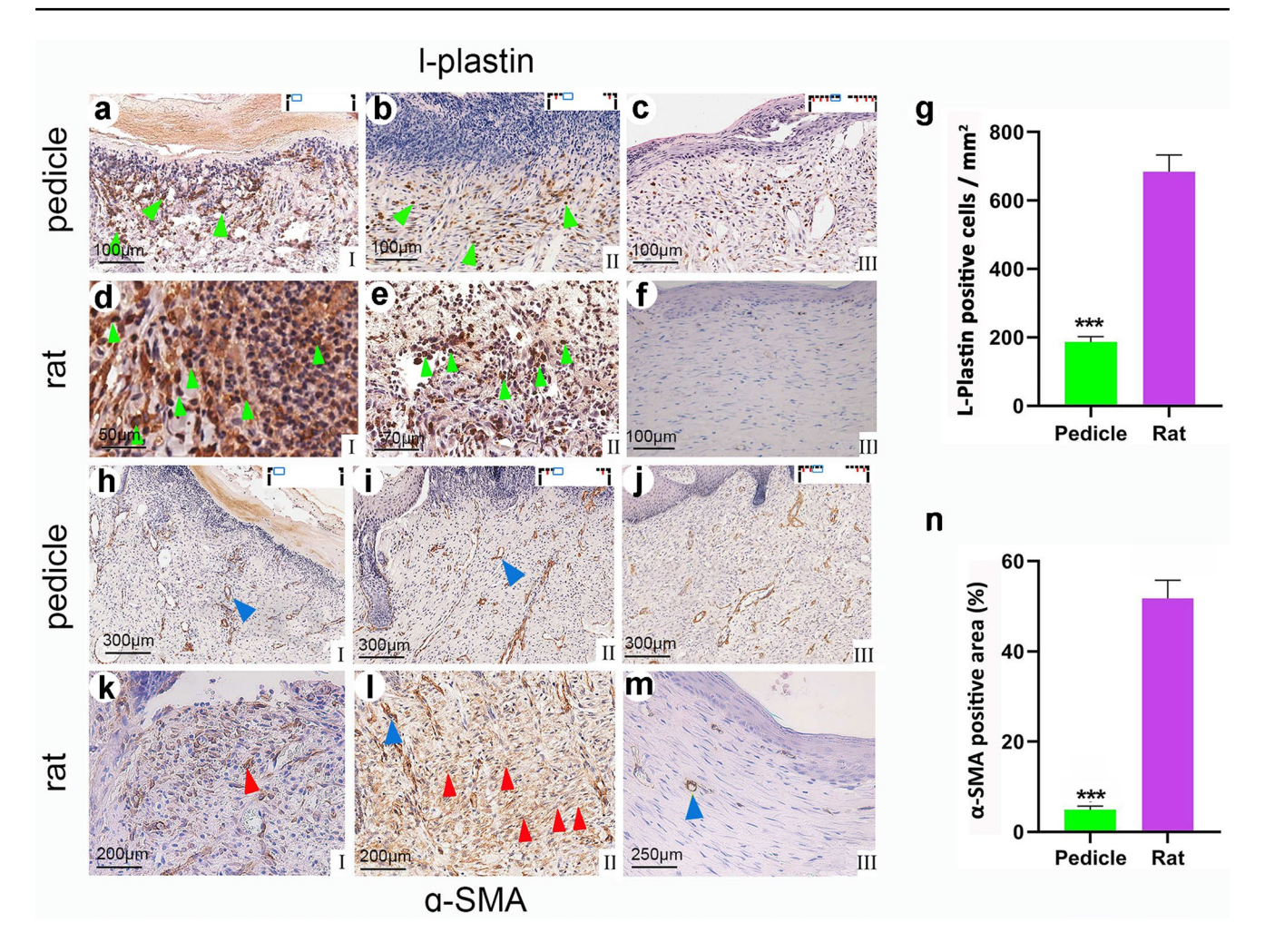


**Fig. 3** Pedicle wound healing exhibits impaired inflammatory response and lacks myofibroblast differentiation compared to the rat cutaneous wounds. Cells of hemopoietic lineages were detected using immunostaining of L-plastin (**a**–**f**) on the wound bed at different time points. An influx of leukocytes was observed in phase I after pedicle wounding but any change in the number of leukocytes was not significant during the rest of the course of healing (**a**–**c**). In contrast, the number of leukocytes was significantly higher in phase I on rat healing beds (**d**) than on pedicle wound beds (**a**). In phase III, leukocytes were hardly detectable (**f**). Total leukocytes counted per mm<sup>2</sup> on the wound bed on phase I were quantified (**g**). Note that leukocyte number after wounding in pedicle was significantly lower than that in rat

(\*\*\*p<0.001). Myofibroblasts were detected on the wound bed using α-SMA immunostaining at different time points of healing (**h**-**m**). No evidence of myofibroblasts was detected on the wound bed during the course of wound healing in pedicle (**h**-**j**). Blue arrows indicated blood vessels. In contrast, strong staining for myofibroblasts was detected in rat (red arrow), especially at phase II (**l**). Positive cell area analysis (α-SMA staining) at phase II using Image-Pro Plus (**n**). Note that myofibroblast numbers after wounding in pedicle were significantly lower than those in rat (\*\*\*p<0.001). Insets show the relative wound position of the pictured tissue. Scale bars = 100 μm (**a**-**c**, **f**), 50 μm (**d**), 70 μm (**e**), 300 μm (**h**-**j**), 200 μm (**k**, **l**), 250 (**m**)

small amount of Col III in the healing tissue on a pedicle wound at phase II (Fig. 4a–a'). Associated with progression of re-epithelialization, the amount of Col III increased significantly; at phase III, a large amount of Col III was observed throughout the healing dermis and this level was maintained thereafter (Fig. 4b–b'). In contrast in the rats (Fig. 4c–c'), Col III started to appear at phase II and then was slowly replaced by Col I. At phase III, Col I completely dominated the healing tissue and was arranged in a dense parallel bundle fashion (Fig. 4d–d'). Our results demonstrate

a major difference in the ratio of Col III/Col I between the healing pedicle stump and rat FTE wounds, with the pedicle healing being more akin to fetal wound healing.

Periodic acid Schiff (PAS) staining was performed to compare BM formation status in the healing tissues of the pedicle stump and rat wounds. The results showed that BM formation was at the same pace along with the re-epithelialization in both pedicle stump and rat wounds (Fig. 4e–h). There was essentially no difference between wound healing in the two tissue types in this regard.



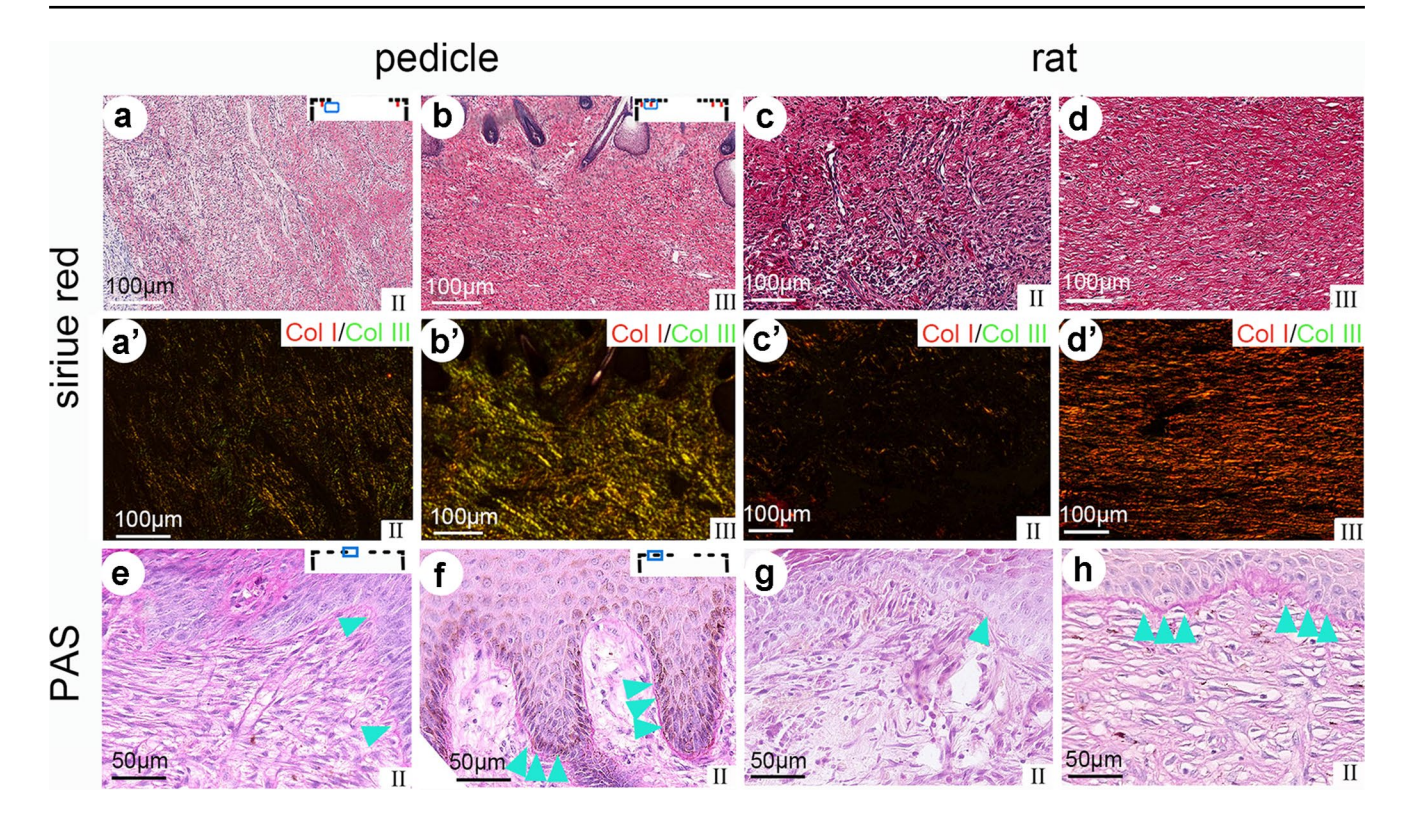


Fig. 4 Healing tissue of pedicle wounds contains more type III collagen (Col), and had well-regenerated basement membrane (BM) at the same pace with the progression of re-epithelialization, just like that in rat wounds. Col I (red/orange) and Col III fibers (green fibers) were discriminated via Picrosirius red staining under polarized light microscope in the healing tissue at different time points (a-d, a'-d'). In phase II, thin collagen fibers were observed in the healing skin of pedicle (a-a') and rat (c-c'). In phase III, abundant fibers were

detected throughout the extracellular matrix (ECM) with a greater proportion of Col III in pedicle ( $\mathbf{b}$ - $\mathbf{b}$ ), and a greater proportion of Col I in rat ( $\mathbf{d}$ - $\mathbf{d}$ '). Periodic acid Schiff (PAS) staining shows regenerated BM ( $\mathbf{e}$ - $\mathbf{h}$ ). In phase II, visible and intact BM (blue arrow) were seen in the interface between the epidermis and dermis in both the pedicle ( $\mathbf{e}$ - $\mathbf{f}$ ) and rat ( $\mathbf{g}$ - $\mathbf{h}$ ), along with the completion of re-epithelialization. Insets show the relative wound position of the pictured tissue. Scale bars = 100  $\mu$ m ( $\mathbf{a}$ - $\mathbf{d}$ ;  $\mathbf{a}$ '- $\mathbf{d}$ '), 50  $\mu$ m ( $\mathbf{e}$ - $\mathbf{h}$ )

### Expression status of healing-relevant genes in pedicle wound favors regeneration

To study the nature of healing at the molecular level in both pedicle stump and rat wounds, we examined expression levels of genes relevant to wound healing, namely TGF-β1 and TGF-β3 through IHC. Results showed that in the pedicle wounds, TGF-β1 positive cells were found only rarely in the healing fibrous tissue at phase I  $(0.0013 \pm 0.0009\%)$ after wounding and were slightly higher  $(0.016 \pm 0.004\%)$ at phase II (Fig. 5a-b"). By contrast in the rat wounds, there were significantly more TGF-\beta1 positive cells  $(0.033 \pm 0.003\%$  at phase I,  $0.070 \pm 0.009\%$  at phase II; Fig. 5i; p < 0.001). TGF- $\beta$ 3-positive cells were detected in the healing tissues of both types of the wounds (Fig. 5e-h''). Results of statistical analysis showed that TGF-β3-positive cells in the healing tissues of pedicle wounds  $(41.7 \pm 1.45\%)$  at phase I,  $30.3 \pm 1.86\%$  at phase II) were significantly higher than those in rat wounds  $(28.0 \pm 1.73\%$  at phase I,  $9.0 \pm 1.16\%$  at phase II) at both phases (Fig. 5j; p < 0.001). Overall, in contrast to the rat wound healing, TGF- $\beta$ 1 gene was downregulated and TGF- $\beta$ 3 gene upregulated in pedicle healing; that is, the ratio of TGF- $\beta$ 3/TGF- $\beta$ 1 was increased, a situation reminiscent of fetal wound healing.

Next, we measured levels of cytokines and chemokines related to the nature of wound healing (that is, regenerative or scar type) in the first 7 days after wounding in the pedicle via cross-species cytokine protein array. The results showed that a rapid induction of expression of inflammatory (th1) cytokines and chemokines occurred on day 1. The level of IFN- $\alpha$  continued to increase and peaked on day 3, and then gradually decreased to the baseline level by day 7 (Fig. 6a). Chemokines IP-10 and MIG were significantly increased on day 1 after wounding, and IP-10 peaked on day 3, whereas MIG leveled off until day 7 (Fig. 6a''). Unexpectedly, in the pedicle healing tissue, we detected high levels of anti-inflammatory



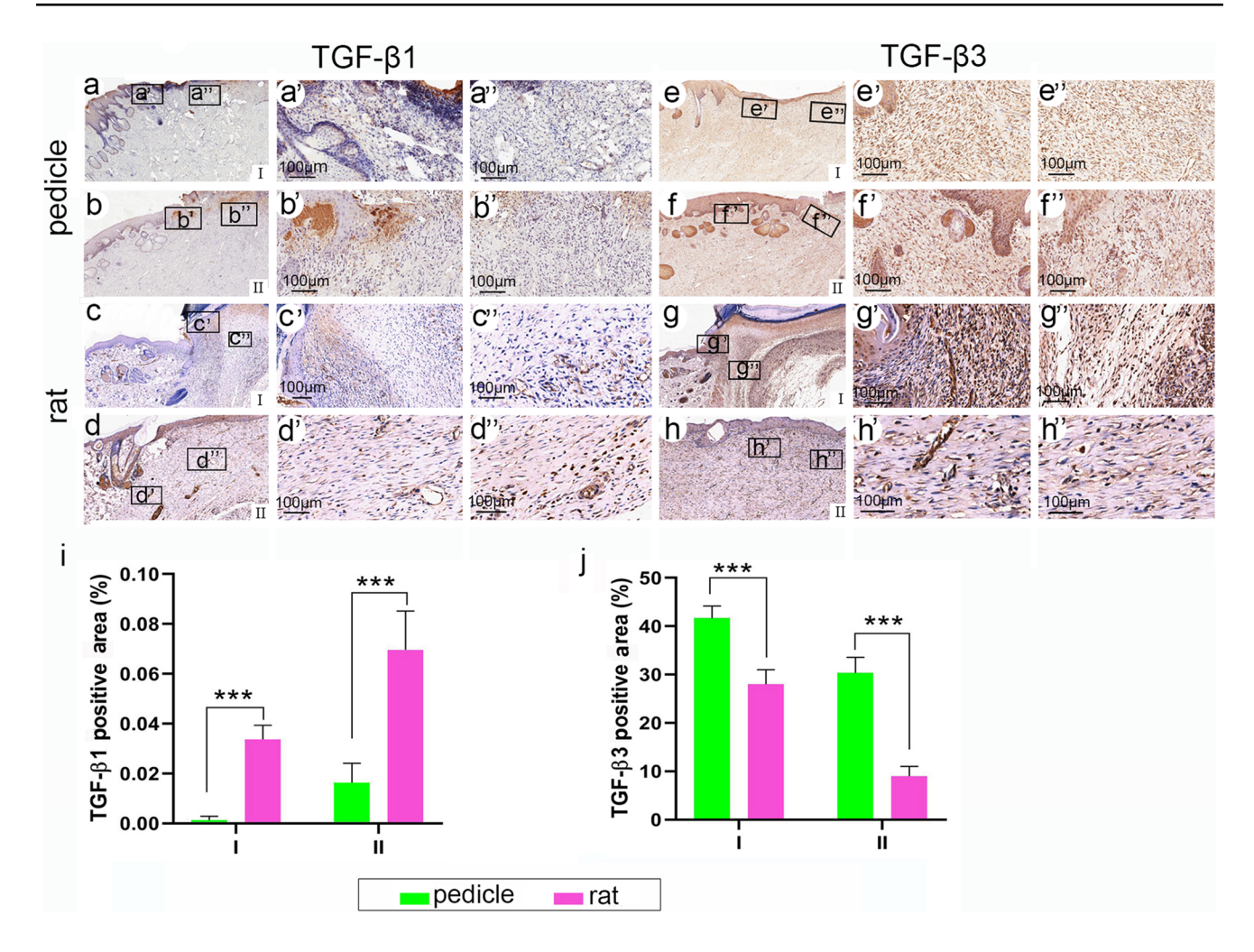


**Fig. 5** Pedicle wound healing exhibits upregulated TGF- $\beta$ 3 and downregulated TGF- $\beta$ 1 compared to rat wounds. TGF- $\beta$ 1 expression in the healing tissue on phases I and II (**a-d''**). TGF- $\beta$ 3 expression in the healing tissue on phases I and II (**e-h''**). Positively stained cell areas of TGF- $\beta$ 1 and TGF- $\beta$ 3 analyzed using Image-Pro Plus (**i-j**). Note that TGF- $\beta$ 1 expression level in the healing tissue over a pedicle

stump wound was significantly lower than that in rat, irrespective of in which phase (\*\*\*p<0.001). In contrast, expression level of TGF- $\beta$ 3 in the healing tissue of a pedicle stump wound was significantly higher than that in rats, irrespective of in which phase (\*\*\*p<0.001). Scale bars = 100  $\mu$ m (a'-h', a''-h'')

(th2) cytokines at the early stage of pedicle wound healing (Fig. 6a'), which are normally induced later in mammalian wound healing (Delavary et al. 2011; Godwin et al. 2013). Expression of IL-1F5 was induced as early as day 1 after wounding and continued to be upregulated in the first 7 days. The expression level of IL-13 peaked on day 3 and remained high thereafter. These results suggest the unusually early activation and high expression of anti-inflammatory cytokines in the pedicle wounds.

In addition, we examined the gene expression status of matrix metalloproteinase (MMP) family members, the tissue inhibitors of metalloproteinases (TIMP), and growth factors (IGF1, VEGF, PDGF-B) during the course of wound healing over a pedicle stump. The results of

mRNA expression analysis (Fig. 6b–d) showed that MMP1, MMP2, and MMP9 exhibited strong upregulation and peaked on day 3, relative to baseline expression in unwounded pedicle skin tissue (day 0). In contrast, expression of TIMP1 and TIMP2 was strongly downregulated on day 1, upregulated on day 3, and then downregulated again on day 5 (Fig. 6e, f), indicating an increase in the ratio of MMPs/TIMPs. Expression levels of growth factors changed significantly following wounding (Fig. 6g–i), especially IGF1 and PDGF-B, with the former being persistently upregulated and the latter significantly downregulated. On day 5, the expression level of IGF1 was upregulated nearly tenfold, while that of PDGF-B was downregulated around tenfold, indicating that the



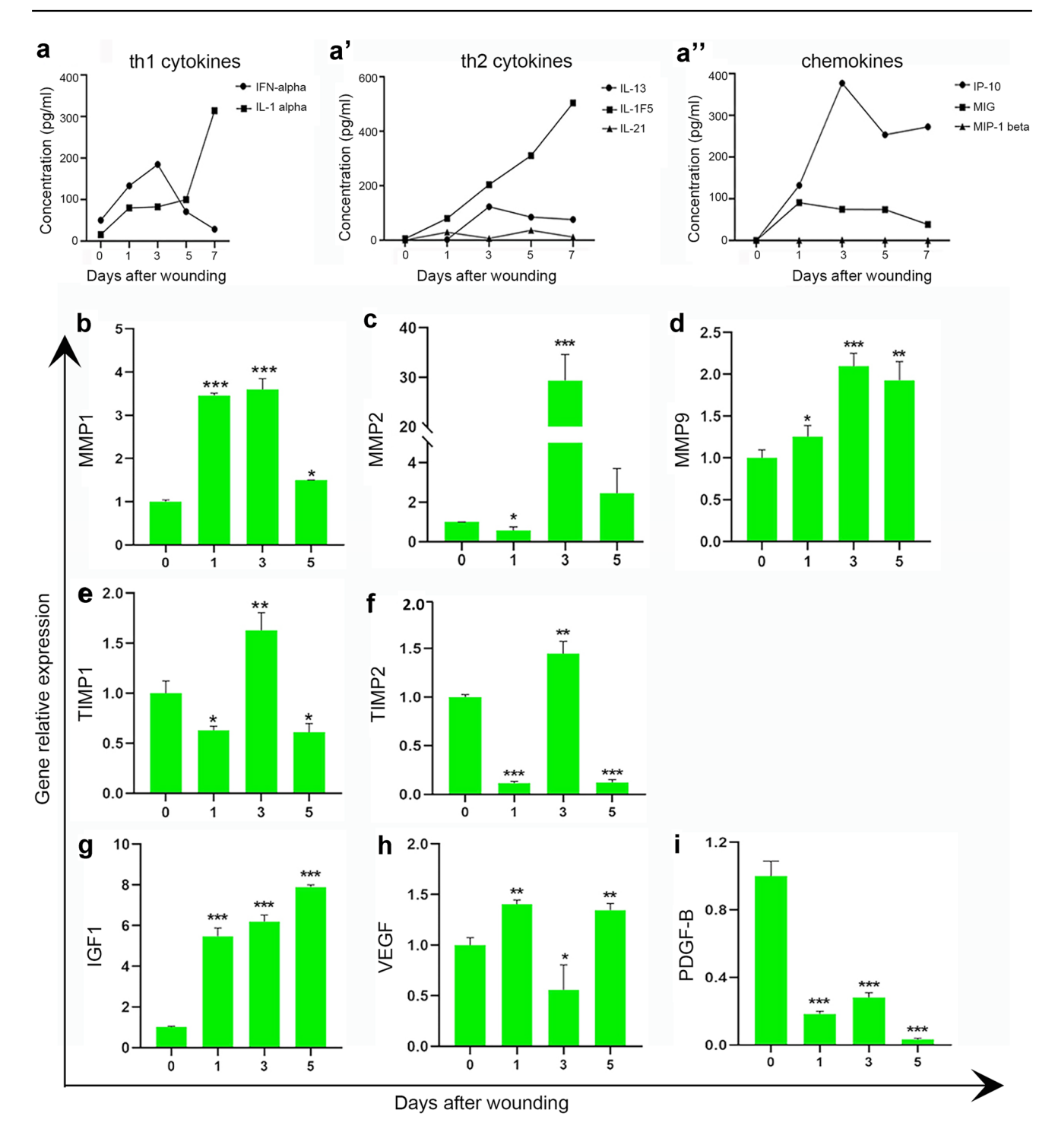


**Fig. 6** Expression status of cytokines (**a-a''**) and genes (**b-i**) related to healing of pedicle wounds favors regeneration. An increased expression in anti-inflammatory (th2) cytokine occurred (**a'**). Changes in cytokine/chemokine expression levels in the healing tissues sampled at various time points relative to the baseline expression in uninjured normal tissue (day 0) were detected using a cross-species cytokine protein array. Evaluation of relative expression levels of MMP1, MMP2, MMP9, TIMP1, TIMP2, IGF1, VEGF, and PDGF-

B mRNAs (**b-i**). Expression status for the selected genes was as follows: (1) strong upregulation during the course of healing with the peak reached on day 3 (MMP1, MMP2, MMP9) or gradual increase (IGF1); (2) strong downregulation on day 1 followed by an equally strong upregulation on day 3 and downregulation on day 5 (TIMP1, TIMP2, PDGF-B); and (3) upregulation on day 1 followed by downregulation on day 3 and then upregulation again on day 5 (VEGF). \*p<0.05, \*\*p<0.01, \*\*\*p<0.001



expression profiles of both growth factors may play key roles in regenerative healing over a pedicle stump wound.

# Exploration of signaling pathways and gene expression status in pedicle wound healing via comparative RNA-seq

To gain further insights into the molecular mechanisms underlying pedicle regenerative wound healing and to look for novel signaling pathways and genes, we performed RNAseq for the healing skin sampled on day 3 after wounding and compared with intact pedicle skin. On day 3, wound healing was well advanced with regenerated skin adorned with hair follicles and sebaceous glands and a number of large blood vessels, which were also seen at the boundary between the regenerated and unwounded skin (Fig. 7a). The RNAseq results showed that at the early stage of wound healing, 403 genes were upregulated and 1226 genes downregulated (Fig. 7b). The Metascape platform (Zhou et al. 2019) was used for GO annotation analysis and KEGG pathway analysis for the differentially expressed genes (DEGs). As shown in Fig. 7c, the upregulated DEGs were significantly enriched in the following biological processes: extracellular matrix organization, blood vessel development, response to growth factor, endothelial cell activation, chemotaxis, which are all related to wound healing. In addition, protein interaction network was analyzed using all upregulated DEGs (Fig. 7e), and two specific module substructures were identified from the interconnection network (Fig. 7f; Table S2): MCODE 1 is found to be involved in the regulation of IGF transport including in being uptaken by IGF binding protein (IGFBP), with the key targets involved in this MCODE being IGFBP4, PAPP-A, and IGFALS. MCODE 2 is found to be involved in anti-inflammatory cytokine production, which might be associated with the high expression of Th2 cytokines at the early stage of pedicle wound healing; targets include RXFP2, HTR7, and GPR176.

### Antler stem cells (ASCs) underpin the regenerative healing over a pedicle stump wound

To investigate the role that ASCs play in pedicle wound healing, we subcutaneously transplanted antlerogenic periosteum (AP) tissue to the deer forehead region, a site where skin can form only a scar when wounded. A pedicle-shaped protuberance formed at the graft site (Fig. 8a), an antler that was initiated from the protuberance went through a normal regenerative cycle, and the hard antler cast off in the following spring, leaving an ectopic pedicle stump wound (Fig. 8b). Morphologically, the wound healed completely within 1 week. Histological examination (Fig. 8e) showed that consistent with the pedicle wound at the original place, the ectopic pedicle wound healing was also regenerative,

including regeneration of dermal tissue, hair follicle, and sebaceous gland. These results suggest that skin of ectopic pedicle, derived from the scalp, acquired regenerative healing ability when it became associated with the AP within which ASCs reside.

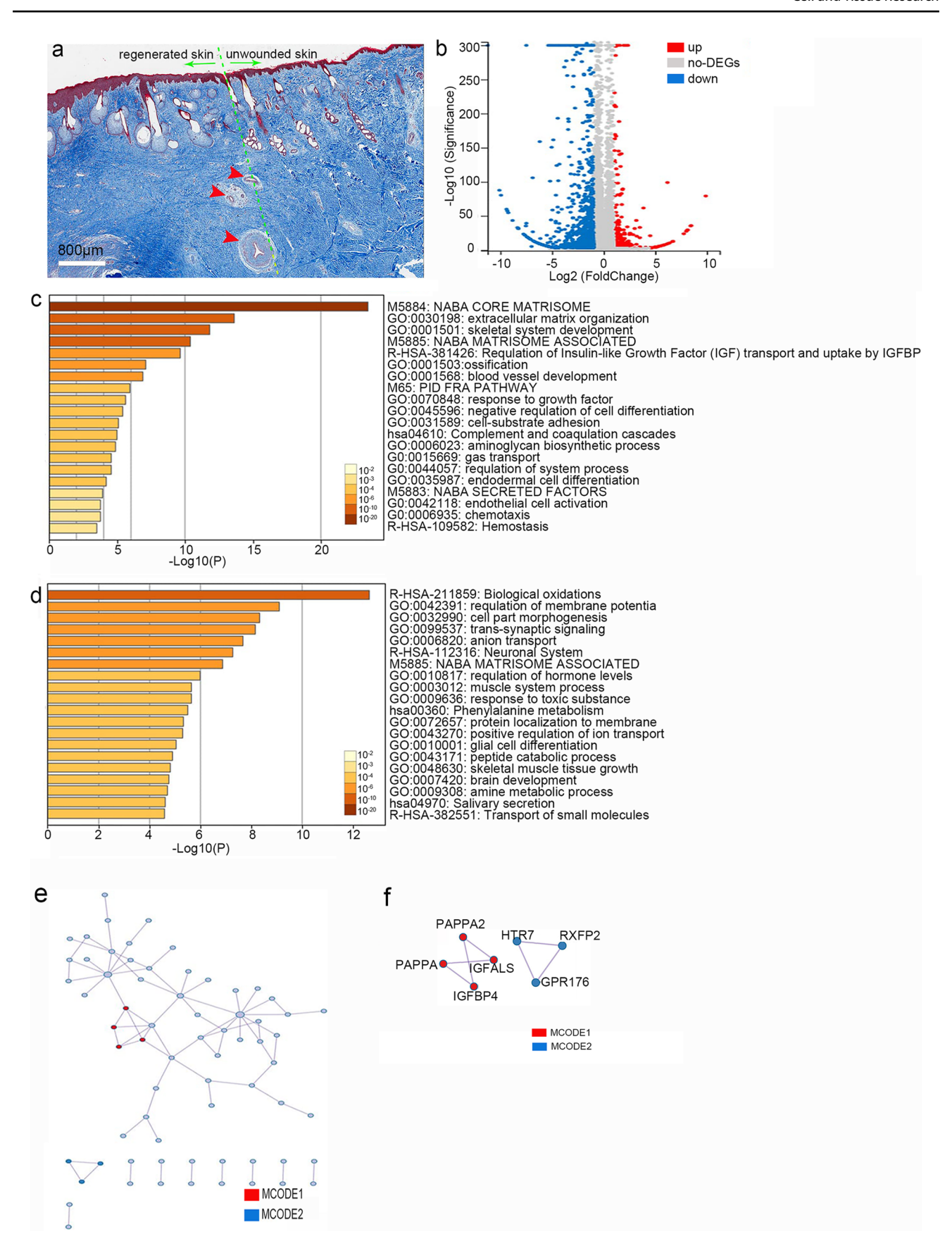
### Transplantation of ASCs induces cutaneous regenerative healing in a rat FTE model

To determine whether the effects of ASCs on promoting regenerative healing are species-specific, experiments with transplantation of the ASCs were performed using a rat FTE model. Representative images of the wound healing skin at different time points (n=3) are shown in Fig. 8f. The rate of wound closure (Fig. 8g) was significantly accelerated in the ASC group as compared with that in the control group. Healed skin was harvested for histological analysis to evaluate the quality of healing (Fig. 8h-o). Numerous regenerated hair follicles and sebaceous glands were observed in the ASC group, in sharp contrast to the control group, in which only very few hair follicles were seen at the wound margin (Fig. 8h-j'). Masson's trichrome staining and analysis was carried out to depict the pattern of collagen deposition. As shown in Fig. 8k-m', collagen fibers (bright blue and thicker diameter) in the ASC group were more mature than those in the control group and were closer to the normal skin. Furthermore, collagen fibers in the ASC group were arranged in a basket-weave-like orientation, typical of unwounded dermis, while those in the control group were arranged in parallel bundles, typical of scar tissue. Quantitative analysis showed that the numbers of hair follicles and sebaceous glands in the ASC group were significantly higher (Fig. 8n), whereas the thickness of both the epidermis and the dermis (Fig. 80) was closer to that of normal skin compared to that in the control group. The results show that the use of ASC treatment in the SD rat model significantly improved the quality of wound healing and promoted skin regeneration.

#### **Discussion**

Deer antlers, bona fide mammalian appendages, are capable of complete regeneration annually, thus offering a unique opportunity to investigate epimorphic regeneration in mammals (Li et al. 2007; He et al. 2018). Antler regeneration starts from wound healing over a pedicle stump. Our study convincingly demonstrates that pedicle wound healing was regenerative in nature, including different developmental stages of skin appendages, and with collagen fibers arranged like a basket weave. Compared to normal mammalian wound repair, the process of pedicle wound healing exhibited weaker inflammatory response and myofibroblast induction with higher ratios of Col III/Col I, TGF $\beta$ 3/TGF $\beta$ 1, and







√Fig. 7 RNA-seq analysis of healed and intact skin tissue. Skin from sampling site of a pedicle stump, stained with Masson's trichrome (a). Differential transcriptome analysis was performed on regenerated and intact skin tissues. The red arrow indicates blood vessels. Differential gene volcano gram (b). 403 genes were upregulated and 1226 genes were downregulated. The Metascape platform was used for GO annotation analysis and the KEGG pathway analysis (c, d) for differentially expressed genes (DEGs). Metascape bar graph for viewing top 20 non-redundant enrichment clusters across upregulated (c) and downregulated (d) differential gene lists, one per cluster, using a discrete color scale to represent statistical significance. Through the Metascape platform, protein-protein interaction enrichment analysis (e) of all upregulated DEGs was carried out. Two MCODE complexes automatically identified in Metascape, colored by their identities. The protein function annotations of the two MCODEs (f) are regulation of IGF transport and uptake by IGF binding protein (IGFBP), and anti-inflammatory cytokine production, respectively. Scale bars =  $800 \mu m (a)$ 

MMP/TIMP. Importantly, our results revealed that this healing process was underpinned by the closely associated deer antler stem cells (ASCs), suggesting that postnatal mammals may retain the ability to deflect the healing toward a regenerative pathway, and that this ability can be activated by factors originating from stem cells. Pedicle wound healing provides an excellent model to study the mechanism of this activation. Interestingly, this regenerative effect of ASCs was found not to be species-specific, as injection of ASCs significantly induced rat FTE wounds healed in a regenerative manner. Overall, our results suggest that ASCs may be of potential value in clinics to improve the quality of wound healing.

Current knowledge in relation to regenerative wound healing comes predominantly from studies on the scar-free healing in zebrafish (Richardson et al. 2013), salamander (Seifert et al. 2012; Lévesque et al. 2010), and the mammalian fetus (Larson et al. 2010; Adzick and Longaker 1991). However, zebrafish and salamander are lower vertebrates, distantly related to mammals, with different skin structure and wound-healing processes, so whether they can be appropriately used as the research models of wound healing for human therapy is not known. The mammalian fetus model differs markedly from the adult situation in both the state of the immune system and the uterine environment (Yates et al. 2013; Seifert et al. 2012). Given the above, the fact that pedicle wounds in adult mammals can achieve regenerative healing (see Fig. 9) is more impressive and provides an excellent model to study the underlying mechanism of regenerative wound healing in a natural setting.

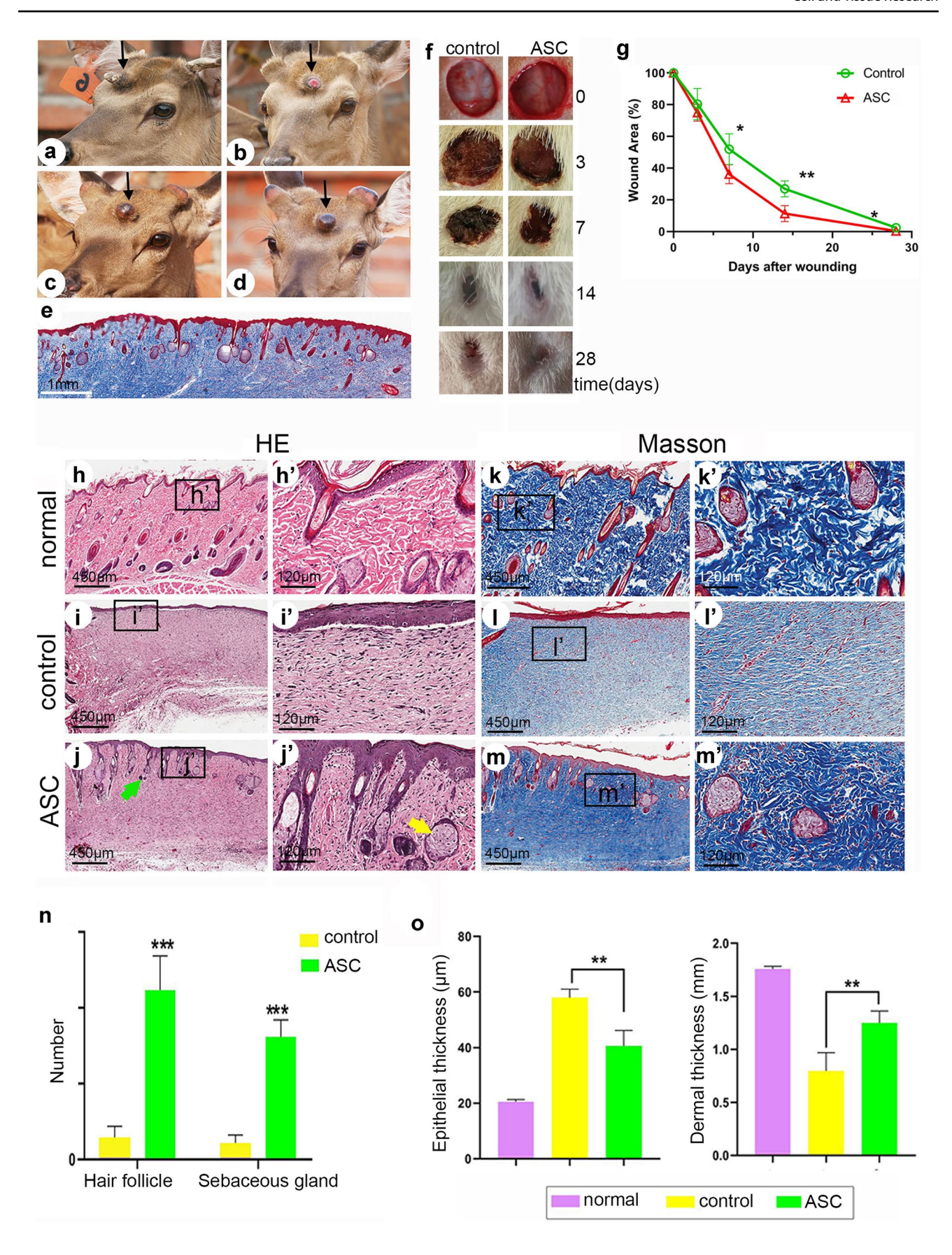
Wound healing is a highly regulated process of cellular, humoral and molecular mechanisms (Yates et al. 2013; Neufeld et al. 1996b), which is generally divided into three distinct but overlapping phases: inflammation, proliferation, and remodeling (Clark et al. 2007). To identify the critical steps in following the regenerative path of wound healing, the major hallmarks of healing over a pedicle stump compared with the

classical scar-based repair observed in most adult mammals and scar-free repair observed in amphibians are summarized in Table 1. In brief, compared with scarred healing in mammals, both regenerative healing over a pedicle stump and scar-free healing in an amphibian showed a low inflammatory response, lack of myofibroblast differentiation, and higher Col III synthesis, indicating that these three characteristics were beneficial for tissue regeneration. Although the currently held notion that reduced inflammation favors regeneration rather than scarring has been popular (Qi et al. 2018; Godwin and Brockes 2006), it raises another question about as to how the animal might resist infections in regenerative environments with weak inflammatory responses. Wound over a pedicle stump can heal regeneratively without becoming infected, offering a unique opportunity to study how infection resistance and regeneration coexist in the future.

In the present study, we examined the expression status of healing-related genes and proteins in the healing tissue of pedicle wounds to investigate possible molecular mechanisms that may antagonize fibrosis and promote regeneration. We found that pedicle wound healing was associated with higher ratios of MMP/TIMP and TGF-β3/TGF-β1, a higher level of IGF1 but a lower level of PDGF-B compared to the scar healing in rats. It is known that fibrosis is associated with the low MMP activity and high TIMP activity (Rohani and Parks 2015; Roderfeld 2018). A high level of TIMP inhibits tissue remodeling, thus promoting scar healing; but high MMPs help to create a niche that allows cells to migrate and proliferate through histolysis, thus favoring regenerative healing. IGF action enhances cell proliferation, survival, and migration of keratinocytes (Chablais and Jazwinska 2010; Edmondson et al. 2003; Semenova et al. 2008). Deficiency in IGF1 is associated with decreased epidermal thickness (Chablais and Jazwinska 2010; Werner and Grose 2003). PDGF-B is reported to regulate wound healing mainly through accelerating healing process and driving fibrosis (Klinkhammer et al. 2018; Barrientos et al. 2014).

From the above, our work demonstrated that regenerative healing of pedicle wounds has unique characteristics involved in all three phases of inflammatory response, proliferation, remolding, and extracellular matrix deposition. Whether these unique characteristics and regenerative outcome of pedicle skin are intrinsic or acquired is not known. Antler generation and annual regeneration have been shown to depend on the presence of periosteal tissue (antlerogenic periosteum and pedicle periosteum) (Li and Chu 2016; Li er al. 2010). Importantly, the cells resident in these periosteal tissues were found to have stem cell attributes, being designated antler stem cells (ASCs) (Wang et al. 2019). Our previous membrane insertion experiments confirmed that close association and interactions between the pedicle periosteum and the enveloping skin are indispensable for







**∢Fig. 8** Antler stem cells (ASCs) underpin regenerative healing over a pedicle stump wound and induce regenerative healing in a rat FTE model. Morphological (a-d) and histological (e) observations of the healing tissue on an ectopic pedicle wound. An ectopic pedicle (arrow) with the attachment of a hard antler (a). Casting of the hard antler in spring created a wound on the ectopic pedicle (b). The wound healed completely within 1 week (c, d). Histological examination of the healed skin via Masson's trichrome staining showed that numerous hair follicles and sebaceous glands were regenerated in the healed skin, and collagen fibers in the dermal tissue were arranged in a basket-weave-like pattern (e). Transplantation of ASCs stimulated regenerative repair to the cutaneous wound in a rat FTE model (f-o). Representative photographs of rat wounds on days 0, 3, 7, 14, and 28 after wounding (f). Wound closure rate in the rat model (g). Healed skin samples from rat collected on day 28 for histological analysis (h-m'). Green and yellow arrows pointed to hair follicles and sebaceous glands respectively. Pattern of collagen deposition in the healed skin and normal skin via Masson's trichrome staining (k-m'). Morphology and pattern of collagen fibers in the ASCs group mostly resemble those of normal skin. Quantification of regenerated hair follicles and sebaceous glands of the healed skin (n). Quantitative analysis of the epithelial and dermal thickness of the healed skin (o). \*p < 0.05, \*\*p < 0.01, \*\*\*p < 0.001. Scale bars = 1 mm (e), 450 µm (h-j, k-m), 120 µm (h'-j',k'-m')

antler regeneration (Li et al. 2011). After the establishment of interactions (already in close contact), the ASCs initiate antler regeneration through exchange of diffusible molecules evidenced by the fact that the use of semi-permeable membrane insertions cannot completely stop the process (Li et al. 2011). Wound healing is the first stage of antler regeneration and it is conceivable that it is the ASCs that have induced this regenerative healing. To test this

hypothesis, we conducted experiments of periosteal transplantation onto deer foreheads and found that the ectopic pedicle wounds perfectly healed after the ectopic hard antler casting, including regeneration of the hair follicles and sebaceous glands. Deer forehead skin can normally form only scar tissue when wounded, but in this case, it acquired the regenerative ability of wound healing when it became associated with the event of antler regeneration. Thus, our data support our hypothesis that the periosteal cells, that is the ASC, fully underpin regenerative wound healing of pedicle.

Our findings lead to the question of species-specificity of the response. Might the ASCs themselves promote regenerative wound healing in the rat (or other mammalian species)? To address this issue, we examined the effects of ASCs on cutaneous wound healing in a rat FTE wound model, and found that systemically injected ASCs effectively promoted regenerative healing in rodents. The ASCs have been defined as a type of mesenchymal stem cells (MSCs) (Wang et al. 2019). Notably, MSCs can be derived from a variety of tissues (Bojanic et al. 2021), such as bone marrow, adipose tissue, and amniotic membrane, and have been widely reported to have the therapeutic potential in enhancing quality of cutaneous wound healing (Cha and Falanga 2007). Although much debate about the mechanism by which MSCs promote tissue wound healing is ongoing, it is generally believed that MSCs could impact wound healing through cell differentiation and release of paracrine factors (Li et al. 2017; Kim et al. 2007). Paracrine effects of MSCs were reported to

**Table 1** The major hallmarks of regenerative tissue repair over a pedicle stump compared with the classic scar-based repair program observed in most adult mammals and scar-free repair observed in salamander

#### **Inflammatory stage** Proliferative/remodeling stage Deer pedicle (regenerative wound healing) • Epithelial/keratinocyte migration occurs under • Basement membrane are restored during early the clotted scab; stages of wound healing; Low level of leukocytes infiltration; Lack myofibroblast induction; •Early expression of anti-inflammatory (Th2) • Rich in collagen III even in the late stage of wound healing Mammalian (scar wound healing) • Epithelial/keratinocyte migration occurs under · Basement membrane are restored during the clotted scab (Godwin et al. 2014); early stages of wound healing (Midwood et al. High level of leukocytes infiltration (Schefe 2004); · Conversion of fibroblasts to myofibroblasts et al. 2006); • Strong inflammatory response (Gurtner et al. 2008); · Collagen III is transformed into collagen I at the later stage of wound healing (Godwin et al. • Basement membrane formation is delayed Salamander (scar-free wound healing) • Epithelial/keratinocyte migration occurs over the clot (Seifert et al. 2012); (Seifert et al. 2012; Neufeld et al. 1996a); • Low level of leukocytes infiltration (Godwin Collagen I synthesis and crosslinking are et al. 2014); delayed (Godwin et al. 2014; Neufeld et al. • Early infiltration of macrophages (Godwin 1996a) et al. 2013) • Lack myofibroblast induction (Lévesque et al. 2010); • Rich in collagen III (Godwin et al. 2014)



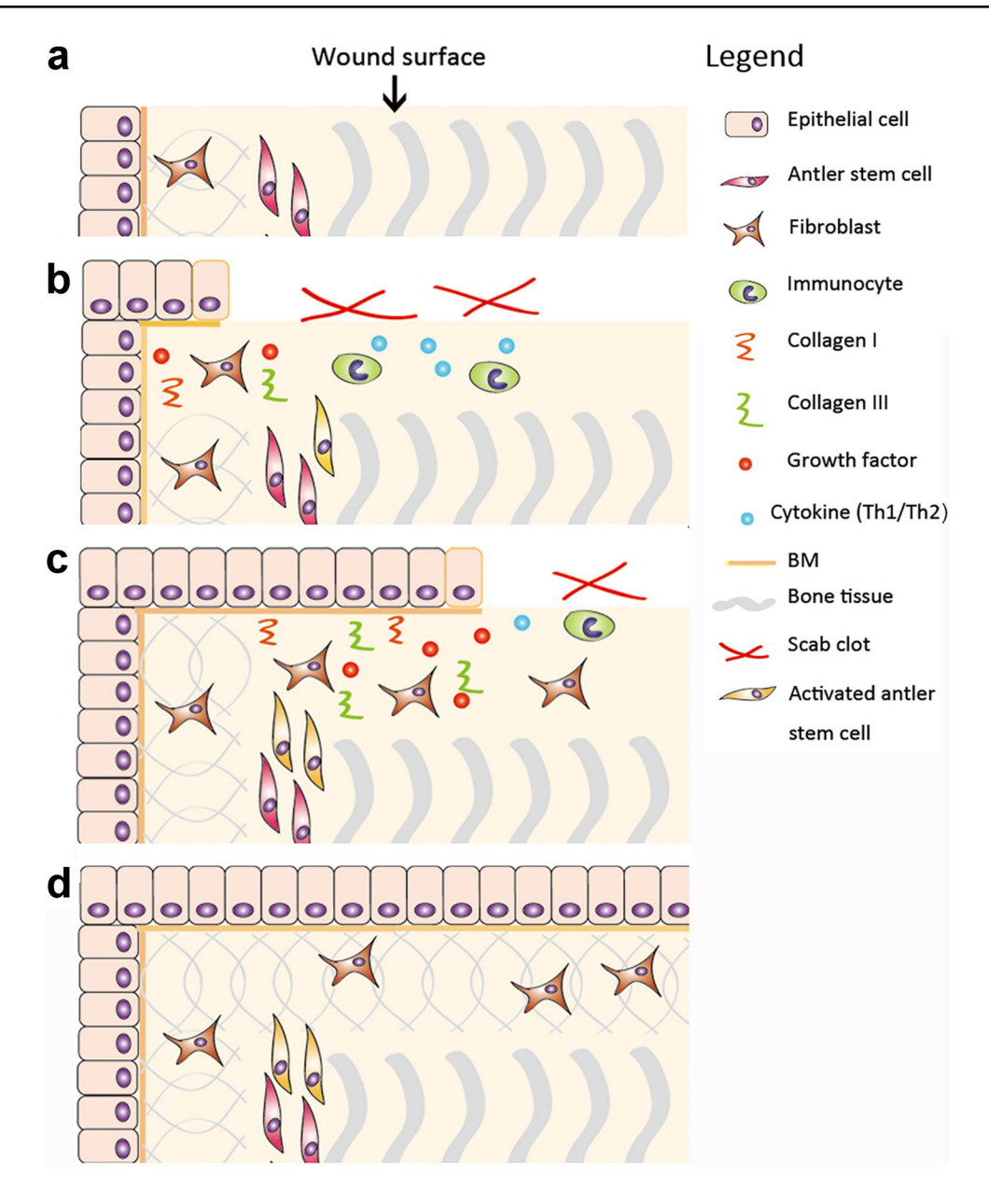


Fig. 9 Schematic diagram to depict the course of regenerative wound healing over a pedicle stump. A large wound formed after hard antler casting (a). Normally uninjured distal pedicle skin was sparsely populated with dermal fibroblasts and closely attached to the pedicle periosteum (PP), where ASCs resided. Immediately, bleeding occurred and a blood scab formed to cover the cast surface of the pedicle stump (b). Immunocytes infiltrated and cytokines and chemokines were secreted in response to wounding. Notably, anti-inflammatory cytokines were produced in the early healing phase. Epithelial cells proliferated to migrate centripetally. Basement membrane was reestablished together with the migrating epidermis. At the same time,

ASCs were in an activated state and had started to proliferate; the process of wound healing towards a regenerative outcome may be via a paracrine effect. Dermal fibroblasts proliferated and migrated centripetally (c). Quite a few types of growth factors, such as IGF1, were secreted into the wound bed by fibroblasts and other dermal cells. The provisional matrix was established and was rich in regeneration-compatible ECM components such as collagen III. Induction of the myofibroblast population was inhibited. The epidermis and dermis were regenerated, including hair follicles and sebaceous glands; the lack of any sign of scar formation is notable (d). The cast surface was totally covered by the newly regenerated cutaneous tissue



promote wound healing, possibly by stimulating the transformation of adult fibroblasts into fetal fibroblasts (Li et al. 2017). Under stimulation of MSC paracrine factors, adult fibroblasts were altered to produce high ratios of Col III/ Col I, TGF- $\beta$ 3/TGF- $\beta$ 1, and MMPs/TIMPs, typical of fetal fibroblasts (Kim et al. 2007; Zhao et al. 2013). In our study, the process of pedicle wound healing exhibited the same characteristics under the regulation of ASCs, suggesting that the mechanism by which ASCs induced regenerative wound healing in both the pedicle and rat wounds may be through promotion of conversion of an adult wound niche into a fetal one. Overall, the evidence is that ASCs may have a profound therapeutic potential in promoting tissue regeneration and preventing scar formation.

#### **Conclusion**

In summary, we have demonstrated that healing of the large wounds over the distal ends of pedicles at the initial stage of antler regeneration is regenerative in nature, and this healing resulted from induction of the pedicle periosteum (a tissue in very close contact), within which ASCs for regeneration reside. Although skin scarring and regenerative wound healing involve a comparable sequence of tissue events, there are important differences at the levels of inflammatory response, myofibroblast induction, and extracellular matrix architecture. ASCs may induce skin regeneration by regulating the aforementioned cellular and molecular events. Furthermore, the fact that administration of ASCs exhibited a enhanced regenerative healing process in a rat FTE wound model suggests that effects of ASCs on regenerative wound healing are more generic and can be applied to other mammalian species other than just deer themselves. Further understanding of the molecular mechanisms underlying both regenerative wound healing of the pedicle and of rat driven by ASCs could lead to development of new therapeutics for regenerative wound healing and tissue regeneration.

**Supplementary information** The online version contains supplementary material available at https://doi.org/10.1007/s00441-021-03505-9.

Acknowledgements We would like to thank Dr Peter Fennessy of AbacusBio Limited, Dunedin, New Zealand, for helping review the manuscript, and staff from the Deer Antler Research Group, Institute of Special Wild Economic Animals and Plants, Chinese Academy of Agricultural Sciences, for the help of collection of antler stem cells.

**Author contribution** QG, CL, and HZ conceived and designed the experiment. QG and ZL performed the experiments. JZ, QG, and HZ performed bioinformatics and statistical analyses. QG and CL drafted the manuscript. HZ, JZ, and CL revised the manuscript. All the authors read and approved the final manuscript.

Funding This work was funded by the Technology Development Plan Project of Jilin Province (20200404004YY and 20190304006YY), Provincial Natural Science Foundation of Jilin (2020201031JC), National Natural Science Foundation of China (U20A20403 and 31901058), and National key Research and Development Project (2018YFC1706603-03).

Availability of data and materials The transcriptome sequencing data for deer has been deposited in the Sequence Read Archive (SRA) database (https://www.ncbi.nlm.nih.gov/sra/) under accession number: SRR13407542; SRR13407538; SRR13407541; SRR13407543; SRR13407539; SRR13407540.

#### **Declarations**

Ethics statement This study was approved by the Animal Ethics Committee of Institute of Special Wild Economic Animals and Plants, Chinese Academy of Agricultural Sciences (Permit Number: NO.ISAPSAEC-2020–022).

**Conflict of interest** The authors declare no competing interests.

#### References

Adzick NS, Longaker MT (1991) Animal models for the study of fetal tissue repair. J Surg Res 51:92–125

Akita S (2019) Wound repair and regeneration: mechanisms, signaling. Int J Mol Sci 20:6328

Barrientos S, Brem H, Stojadinovic O, Tomic-Canic M (2014) Clinical application of growth factors and cytokines in wound healing. Wound Repair Regen 22:569–578

Bojanic C, To K, Hatoum A, Shea J, Seah KTM, Khan W, Malata CM (2021) Mesenchymal stem cell therapy in hypertrophic and keloid scars. Cell Tissue Res. https://doi.org/10.1007/s00441-020-03361-z

Brown BC, McKenna SP, Siddhi K, McGrouther DA, Bayat A (2008) The hidden cost of skin scars: quality of life after skin scarring. J Plast Reconstr Aesthet Surg 61:1049–1058

Cha J, Falanga V (2007) Stem cells in cutaneous wound healing. Clin Dermatol 25:73–78

Chablais F, Jazwinska A (2010) IGF signaling between blastema and wound epidermis is required for fin regeneration. Development 137:871–879

Clark RA, Ghosh K, Tonnesen MG (2007) Tissue engineering for cutaneous wounds. J Invest Dermatol 127:1018–1029

Delavary BM, van der Veer WM, van Egmond M, Niessen FB, Beelen RHJ (2011) Macrophages in skin injury and repair. Immunobiology 216:753–762

Delorme SL, Lungu IM, Vickaryous MK (2012) Scar-free wound healing and regeneration following tail loss in the Leopard Gecko, Eublepharis macularius. Anat Rec 295:1575–1595

Edmondson SR, Thumiger SP, Werther GA, Wraight CJ (2003) Epidermal homeostasis: the role of the growth hormone and insulin-like growth factor systems. Endocr Rev 24:737–764

Eming SA, Martin P, Tomic-Canic M (2014) Wound repair and regeneration: mechanisms, signaling, and translation. Sci Transl Med 6:265sr6 Falcon S, Gentleman R (2007) Using GOstats to test gene lists for GO term association. Bioinformatics 23:257–258

Gurtner GC, Werner S, Barrandon Y, Longaker MT (2008) Wound repair and regeneration. Nature 453:314–321

Goss RJ (1995) Future directions in antler research. Anat Rec 241:291-302

Goss RJ (1983) Chondrogenesis in regenerating systems. In: Hall B (ed) Cartilage: biomedical aspects. Academic Press, New York, pp 267–370



- Godwin JW, Pinto AR, Rosenthala RNA (2013) Macrophages are required for adult salamander limb regeneration. PNAS 110:9415-9420
- Godwin J, Kuraitis D, Rosenthal N (2014) Extracellular matrix considerations for scar-free repair and regeneration: insights from regenerative diversity among vertebrates. Int J Biochem Cell Biol 56:47–55
- He Y, Fischer D, Hasan I, Götz W, Keilig L, Ziegler L, Abboud M, Bourauel C, Wahl G (2018) Sika deer antler as a novel model to investigate dental implant healing: a pilot experimental study. PLoS One 13:e0200957. https://doi.org/10.1371/journal.pone.0200957
- Godwin JW, Brockes JP (2006) Regeneration, tissue injury and the immune response. J Anat 209:423–432
- Kierdorf U, Stoffels E, Stoffels D, Kierdorf H, Szuwart T, Clemen G (2003) Histological studies of bone formation during pedicle restoration and early antler regeneration in roe deer and fallow deer. Anat Rec 273A:741–751
- Kim WS, Park BS, Sung JH, Yang JM, Park SB, Kwak SJ, Park JS (2007) Wound healing effect of adipose-derived stem cells: a critical role of secretory factors on human dermal fibroblasts. J Dermatol Sci 48:15–24
- Klinkhammer BM, Floege J, Boor P (2018) PDGF in organ fibrosis. Mol Asp Med 62:44–62
- Larson BJ, Longaker MT, Lorenz HP (2010) Scarless fetal wound healing: a basic science review. Plast Reconstr Surg 126(4):1172–1180
- Lévesque M, Villiard É, Roy S (2010) Skin wound healing in axolotls: a scarless process. J Exp Zool 314B:684–697
- Li C, Suttie JM (1994) Light microscopic studies of pedicle and early first antler development in red deer (Cervus elaphus). Anat Rec 239:198–215
- Li C, Suttie JM (2001) Deer antlerogenic periosteum: a piece of postnatally retained embryonic tissue? Anat Embryol (Berl) 204:375–388
- Li C, Suttie JM (2003) Tissue collection methods for antler research. Eur J Morphol 41:23–30
- Li C, Mackintosh CG, Martin SK, Clark DE (2007) Identification of key tissue type for antler regeneration through pedicle periosteum deletion. Cell Tissue Res 328:65–75
- Li C, Suttie JM, Clark DE (2005) Histological examination of antler regeneration in red deer (Cervus elaphus). Anat Rec A Discov Mol Cell Evol Biol 282A:163–174
- Li C, Chu WH (2016) The regenerating antler blastema: the derivative of stem cells resident in a pedicle stump. Front Biosci (Landmark Ed) 21:455–467
- Li C, Yang FH, Suttie J (2011) Stem cells, stem cell niche and antler development. Anim Prod Sci 51:267–276
- Li C, Yang F, Sheppard A (2009) Adult stem cells and mammalian epimorphic regeneration-insights from studying annual renewal of deer antlers. Curr Stem Cell Res Ther 4:237–251
- Li C, Yang F, Haines S, Zhao H, Wang W, Xing X, Sun H, Chu W, Lu X, Liu L, McMahon C (2010) Stem cells responsible for deer antler regeneration are unable to recapitulate the process of first antler development—revealed through intradermal and subcutaneous tissue transplantation. J Exp Zool 314:552–570
- Li M, Luan F, Zhao Y, Hao H, Liu J, Dong L, Fu X, Han W (2017) Mesenchymal stem cell-conditioned medium accelerates wound healing with fewer scars. Int Wound J 14:64–73
- Midwood KS, Williams LV, Schwarzbauer JE (2004) Tissue repair and the dynamics of the extracellular matrix. Int J Biochem Cell Biol 36:1031–1037
- Moeini A, Pedram P, Makvandi P, Malinconico M, Gomez d'Ayala G (2020) Wound healing and antimicrobial effect of active secondary metabolites in chitosan-based wound dressings: a review. Carbohydr Polym. https://doi.org/10.1016/j.carbpol.2020.115839
- Namazi MR, Feily A (2011) Homocysteine may accelerate skin aging: a new chapter in the biology of skin senescence? J Am Acad Dermatol 64:1175-1178

- Neufeld DA, Day FA, Perspective, (1996a) A suggested role for basement membrane structures during newt limb regeneration. Anat Rec 246:155–161
- Neufeld DA, Day FA, Settles HE (1996b) Stabilizing role of the basement membrane and dermal fibers during newt limb regeneration. Anat Rec 245:122–127
- Olczyk P, Mencner Ł, Komosinska-Vassev K (2014) The role of the extracellular matrix components in cutaneous wound healing. Biomed Res Int. https://doi.org/10.1155/2014/747584
- Peacock HM, Gilbert EA, Vickaryous MK (2015) Scar-free cutaneous wound healing in the leopard gecko, Eublepharis macularius. J Anat 227:596–610
- Price J, Faucheux C, Allen S (2005) Deer antlers as a model of Mammalian regeneration. Curr Top Dev Biol 67:1–48
- Qi K, Li N, Zhang Z, Melino G (2018) Tissue regeneration: the crosstalk between mesenchymal stem cells and immune response. Cell Immunol 326:86–93
- Reinke JM, Sorg H (2012) Wound repair and regeneration. Eur Surg Res 49:35–43
- Richardson R, Slanchev K, Kraus C, Knyphausen P, Eming S, Hammerschmidt M (2013) Adult zebrafish as a model system for cutaneous wound healing research. J Invest Dermatol 133:1655–1665
- Rohani MG, Parks WC (2015) Matrix remodeling by MMPs during wound repair. Matrix Biol 44–46:113–121
- Roderfeld M (2018) Matrix metalloproteinase functions in hepatic injury and fibrosis. Matrix Biol 68–69:452–462
- Schefe JH, Lehmann KE, Buschmann IR, Unger T, Funke-Kaiser H (2006) Quantitative real-time RT-PCR data analysis: current concepts and the novel "gene expression's CT difference" formula. J Mol Med 84:901–910
- Seifert AW, Monaghan JR, Voss SR, Maden M (2012) Skin regeneration in adult axolotls: a blueprint for scar-free healing in vertebrates. PLoS One 7:e32875
- Semenova E, Koegel H, Hasse S, Klatte J, Slonimsky E, Bilbao D, Paus R, Werner S, Rosenthal N (2008) Overexpression of mIGF-1 in keratinocytes improves wound healing and accelerates hair follicle formation and cycling in mice. Am J Pathol 173:1295–1310
- Shaw TJ, Martin P (2016) Wound repair: a showcase for cell plasticity and migration. Curr Opin Cell Biol 42:29–37
- Stoica AE, Grumezescu AM, Hermenean AO, Andronescu E, Vasile BS (2020) Scar-free healing: current concepts and future perspectives. Nanomaterials (basel) 10:2179
- Takeo M, Lee W, Ito M (2015) Wound healing and skin regeneration. Cold Spring Harb Perspect Med 5:a02326
- Wang DT, Berg D, Ba HX, Sun HM, Wang Z, Li C (2019) Deer antler stem cells are a novel type of cells that sustain full regeneration of a mammalian organ—deer antler. Cell Death Dis 10:443
- Werner S, Grose R (2003) Regulation of wound healing by growth factors and cytokines. Physiol 83:835–870
- Yates CC, Hebda P, Wells A (2013) Skin wound healing and scarring: fetal wounds and regenerative restitution. Birth Defects Res C 96:325–333
- Zhao J, Hu L, Liu J, Gong N, Chen L (2013) The effects of cytokines in adipose stem cell-conditioned medium on the migration and proliferation of skin fbroblasts in vitro. BioMed Res Int. https://doi.org/10.1155/2013/578479
- Zhou Y, Zhou B, Pache L, Chang M, Khodabakhshi AH, Tanaseichuk O, Benner C, Chanda SK (2019) Metascape provides a biologistoriented resource for the analysis of systems-level datasets. Nat Commun 10:1523

**Publisher's Note** Springer Nature remains neutral with regard to jurisdictional claims in published maps and institutional affiliations.

